

## SPECTRAL ANALYSIS OF THE DISCRETE HELMHOLTZ OPERATOR PRECONDITIONED WITH A SHIFTED LAPLACIAN\*

M. B. VAN GIJZEN<sup>†</sup>, Y. A. ERLANGGA<sup>‡</sup>, AND C. VUIK<sup>†</sup>

**Abstract.** Shifted Laplace preconditioners have attracted considerable attention as a technique to speed up convergence of iterative solution methods for the Helmholtz equation. In this paper we present a comprehensive spectral analysis of the Helmholtz operator preconditioned with a shifted Laplacian. Our analysis is valid under general conditions. The propagating medium can be heterogeneous, and the analysis also holds for different types of damping, including a radiation condition for the boundary of the computational domain. By combining the results of the spectral analysis of the preconditioned Helmholtz operator with an upper bound on the GMRES-residual norm, we are able to provide an optimal value for the shift and to explain the mesh-dependency of the convergence of GMRES preconditioned with a shifted Laplacian. We illustrate our results with a seismic test problem.

**Key words.** Helmholtz equation, shifted Laplace preconditioner, iterative solution methods, GMRES, convergence analysis

**AMS subject classifications.** 65N55, 65F10, 65N22, 78A45, 76Q05

**DOI.** 10.1137/060661491

**1. Introduction.** In this paper we investigate the spectral behavior of iterative methods applied to the time-harmonic wave equation in heterogeneous media. The underlying equation governs wave propagation and scattering phenomena arising in acoustic problems in many areas, e.g., aeronautics, marine technology, geophysics, and optical problems. In particular, we look for solutions of the Helmholtz equation discretized by using finite difference, finite volume, or finite element discretizations. Since the number of grid points per wavelength should be sufficiently large to result in acceptable solutions, for very high frequencies the discrete problem becomes extremely large, prohibiting the use of direct solution methods. Krylov subspace iterative methods are an interesting alternative. However, Krylov subspace methods are not competitive without a good preconditioner.

Finding a suitable preconditioner for the Helmholtz equation is still an area of active research; see, for example, [7]. A class of preconditioners that has recently attracted considerable attention is the class of shifted Laplace preconditioners. Preconditioning of the Helmholtz equation using the Laplace operator without shift was first suggested in [1]. This approach has been enhanced in [8, 9] by adding a positive shift to the Laplace operator, resulting in a positive definite preconditioner. In [2, 3, 4, 13] the class of shifted Laplace preconditioners is further generalized by also considering general complex shifts.

It is well known that the spectral properties of the preconditioned matrix give important insight in the convergence behavior of the preconditioned Krylov subspace methods. Spectral analyses for the Helmholtz equation preconditioned by a shifted

---

\*Received by the editors May 31, 2006; accepted for publication (in revised form) January 10, 2007; published electronically September 28, 2007. Part of this research was funded by the Dutch BSIK/BRICKS project.

<http://www.siam.org/journals/sisc/29-5/66149.html>

<sup>†</sup>Delft Institute of Applied Mathematics, Delft University of Technology, Mekelweg 4, 2628 CD, The Netherlands (M.B.vanGijzen@tudelft.nl, C.Vuik@tudelft.nl).

<sup>‡</sup>Institut für Mathematik, Technische Universität Berlin, Strasse des 17. Juni 136, D-10623 Berlin, Germany (erlangga@math.tu-berlin.de).

Laplace operator have previously been given in [2, 3, 4]. The analysis in [2], however, is restricted to the homogeneous physical parameters case, for a purely imaginary shift preconditioner. This analysis concerns the singular values of the preconditioned matrix rather than the eigenvalues. Furthermore, only reflecting and pressure release boundary conditions are considered. In [3], a convergence analysis of GMRES is discussed, under the same restriction as in [2]. A more thorough spectral analysis is presented in [4] for the case when the preconditioning operation is performed approximately by using multigrid. The analysis is based on rigorous Fourier analysis (RFA) for homogeneous physical parameters. Results from RFA, however, give little insight into the convergence of Krylov subspace methods.

This paper gives a spectral analysis from an algebraic point of view. Therefore, the results are valid under the following rather general conditions:

- They do not depend on the discretization method;
- inhomogeneous physical parameters (such as sound speed, density, and damping) are allowed;
- the analysis is also valid for various types of boundary conditions (reflecting, radiation, pressure release, and perfectly matched layer (PML) as well).

These generalizations are new, and they allow us to analyze shifted-Laplace preconditioners for a much wider class of discrete Helmholtz problems than in previous publications.

By combining the results of our analysis with a bound on the norm of the GMRES-residual, we are able to derive a “quasi” optimal value for the shift. This result is also new. The shift is derived under the assumption that the preconditioning operations with the shifted-Laplace preconditioner are performed sufficiently accurately. In practice, the preconditioning operations are performed only approximately, for example, by using a multigrid method or by making an ILU decomposition of the shifted-Laplace operator. Of course, our results do not hold unconditionally in these cases. However, the results that are reported in [2, 3, 4], where the preconditioning operations are performed approximately using either a multigrid method or incomplete LU factorization (ILU), are obtained using shifts that are close to the optimal shift that follows from our analysis. This indicates that the optimal shift that we derive in this paper also gives strong guidelines for choosing the shift in the case when the preconditioning operations are performed approximately.

This paper is organized as follows. In section 2 we describe the acoustic wave equation and its discretization. We specify some properties of the matrices (symmetry, complex valued, positive definiteness etc.), which form the coefficient matrix of the resulting linear system. In section 3 we show that for the damped Helmholtz equation with Dirichlet and Neumann boundary conditions, the eigenvalues are located on a line or on a circle with a given parameterization for a special type of damping. For radiation boundary conditions and for general viscous media we show that the eigenvalues are located on one side of the line or within the circle. In section 4 we use a simple bound on the GMRES-residual norm. Using this bound and the results of our spectral analysis we are able to derive the optimal value of the shift in the shifted Laplacian preconditioner. We also show for a number of applications that the convergence of GMRES is independent of the grid size. Section 5 contains numerical experiments to illustrate and verify the theoretical results derived in sections 3 and 4. Finally, section 6 contains the conclusions of this paper.

## 2. The Helmholtz equation.

**2.1. The acoustic wave equation.** An acoustic medium with space-varying density  $\rho(\mathbf{x})$  and sound speed  $c(\mathbf{x})$  occupies the volume  $\Omega$ , bounded by the boundary  $\Gamma = \Gamma_1 \cup \Gamma_2 \cup \Gamma_3$ . In addition, the medium is assumed to be viscous with damping coefficient  $\gamma(\mathbf{x})$ . The wave equation for the acoustic pressure  $p(\mathbf{x}, t)$  (with  $\mathbf{x}$  spatial coordinates and  $t$  time) in such a medium is

$$(1) \quad \frac{1}{\rho c^2} \frac{\partial^2 p}{\partial t^2} + \frac{\gamma}{\rho} \frac{\partial p}{\partial t} - \nabla \cdot \frac{1}{\rho} \nabla p = \frac{s(\mathbf{x}, t)}{\rho} \quad \text{in } \Omega,$$

where  $\nabla$  denotes the gradient operator and  $\nabla \cdot$  the divergence. Realistic conditions on the physical boundaries of an acoustic medium can be reflecting boundaries, which are described by the homogeneous Neumann condition

$$(2) \quad \frac{\partial p}{\partial n} = 0 \quad \text{on } \Gamma_1;$$

pressure release boundaries, which are described by the homogeneous Dirichlet condition

$$(3) \quad p = 0 \quad \text{on } \Gamma_2;$$

and radiating boundaries, which can be described by

$$(4) \quad \frac{\partial p}{\partial n} = -\frac{1}{\rho c} \frac{\partial p}{\partial t} \quad \text{on } \Gamma_3,$$

where  $n$  is the outward pointing normal unit vector.

We will assume that the right-hand side function  $s(\mathbf{x}, t)$  is a harmonic point source  $s(\mathbf{x}, t) = ae^{2\pi i f t} \delta(\mathbf{x} - \mathbf{x}_s)$ , located at  $\mathbf{x}_s$ , which transmits a signal with amplitude  $a$  and frequency  $f$ . Here,  $i = \sqrt{-1}$ .

**2.2. The Helmholtz equation.** If the source term is harmonic, then the pressure field has the factored form

$$(5) \quad p(\mathbf{x}, t) = \hat{p}(\mathbf{x}) e^{2\pi i f t}.$$

Substitution of (5) into (1) yields the so-called Helmholtz equation

$$(6) \quad \left( \frac{-(2\pi f)^2}{\rho c^2} + 2\pi i f \frac{\gamma}{\rho} \right) \hat{p} - \nabla \cdot \frac{1}{\rho} \nabla \hat{p} = \frac{a}{\rho} \delta(\mathbf{x} - \mathbf{x}_s) \quad \text{in } \Omega,$$

with boundary conditions

$$(7) \quad \frac{\partial \hat{p}}{\partial n} = 0 \quad \text{on } \Gamma_1,$$

$$(8) \quad \hat{p} = 0 \quad \text{on } \Gamma_2,$$

and

$$(9) \quad \frac{\partial \hat{p}}{\partial n} = -\frac{2\pi i f}{\rho c} \hat{p} \quad \text{on } \Gamma_3.$$

This latter condition is also known as a Sommerfeld condition of the first kind.

If the damping parameter has the special form

$$(10) \quad \gamma(\mathbf{x}, f) = 2\pi f \frac{\nu}{c^2},$$

with  $\nu$  a nonnegative constant, the Helmholtz equation (6) simplifies to

$$(11) \quad \left( -\frac{(2\pi f)^2}{\rho c^2} (1 - i\nu) - \nabla \cdot \frac{1}{\rho} \nabla \right) \hat{p} = a \frac{\delta(\mathbf{x} - \mathbf{x}_s)}{\rho(\mathbf{x}_s)} \quad \text{in } \Omega.$$

Clearly, the assumption holds for nonviscous media, i.e., with  $\gamma = 0$ .

The above equation can be discretized with a discretization method such as the finite element method, finite volume method, or finite difference method. Discretization of the above equation plus boundary conditions with any of these methods yields a discrete Helmholtz equation of the form

$$(12) \quad (L + iC - z_1 M)x = b$$

in which  $L$  is the discretization of  $-\nabla \cdot \frac{1}{\rho} \nabla$ ,  $M$  corresponds to the discretized zeroth order term  $\frac{1}{\rho c^2}$ ,  $C$  corresponds to the Sommerfeld condition and/or to damping that does not satisfy (10), and  $b$  to the source term. The complex number  $z_1$  is defined by

$$(13) \quad z_1 = (2\pi f)^2 (1 - i\nu).$$

Both  $L$  and  $C$  are real symmetric and positive semidefinite, and the matrix  $M$  is real symmetric and positive definite. The matrix  $L + iC - z_1 M$ , however, is complex symmetric and indefinite.

For high frequencies, system (12) can be very large, in particular in three dimensions. This is a consequence of the fact that each wavelength has to be sampled with sufficient grid points. Numbers of unknowns in excess of  $10^6$  for realistic models are quite common. Fortunately, system (12) is sparse. Krylov-type iterative solvers such as GMRES [12] or Bi-CGSTAB [14] are among the most popular techniques for solving large and sparse linear systems. They have proved to be particularly efficient for systems with an Hermitian positive definite matrix, or more generally, for systems with a matrix with all eigenvalues in the right half of the complex plane. Helmholtz-type systems such as (12), however, are highly indefinite, which means that the system matrix has eigenvalues with both negative and positive real parts, a characteristic that can result in a very slow convergence. In order to overcome this problem a suitable preconditioner has to be applied. A class of promising preconditioners that has attracted a lot of attention is the class of shifted Laplace preconditioners [1, 8, 2, 3, 4]. In the next section we will analyze these preconditioners by locating in the complex plane the spectrum of the preconditioned discrete Helmholtz operator.

**3. Spectral analysis of the Helmholtz operator preconditioned with the shifted Laplace preconditioner.** Shifted Laplace preconditioners are preconditioners of the form

$$P = L + iC - z_2 M,$$

i.e., the same form as the discrete Helmholtz operator  $A = L + iC - z_1 M$ . The shift parameter  $z_2$  has to be chosen such that the convergence of GMRES (or another suitable iterative method) applied to the preconditioned system

$$(L + iC - z_2 M)^{-1} (L + iC - z_1 M)x = (L + iC - z_2 M)^{-1} b$$

is considerably faster than GMRES applied to the original system. Moreover,  $z_2$  has to be chosen such that operations with the inverse of  $(L + iC - z_2M)$  are easy to perform. In practice this means that  $z_2$  is chosen such that operations with the inverse of the preconditioner can be computed using a fast multigrid method [4]. Note that  $L + iC$  is the operator that is being shifted. This means that all boundary conditions, including the Sommerfeld condition, are included in the preconditioner, as recommended in [10].

The complex numbers  $z_1$  and  $z_2$  can be written as

$$(14) \quad z_1 = \alpha_1 + i\beta_1, \quad z_2 = \alpha_2 + i\beta_2,$$

in which  $\alpha_1, \beta_1, \alpha_2$ , and  $\beta_2$  are real. Recall that for our application,  $z_1$  is defined by (13), and hence

$$\alpha_1 > 0, \quad \beta_1 \leq 0.$$

Choices for the shift  $z_2$  that are considered in the literature are  $z_2 = 0$  [1],  $z_2 = -\alpha_1$  [8],  $z_2 = -i\alpha_1$  [2, 3], and  $z_2 = (1 - 0.5i)\alpha_1$  [4].

In this section we will study the spectrum of the preconditioned system. The spectrum governs, to a large extent, the convergence of iterative methods as long as the matrix of the eigenvectors is well conditioned.

**3.1. The spectrum of the preconditioned Helmholtz operator without the Sommerfeld condition.** We will first assume that  $C = 0$ , and hence that the damped Helmholtz operator is given by  $L - z_1M$ . We recall that  $L$  is symmetric positive semidefinite,  $M$  symmetric positive definite, and  $z_1$  is a complex number. We will consider a shifted Laplace preconditioner, i.e., a matrix of the form  $L - z_2M$ , as a preconditioner for the Helmholtz operator and analyze how the location of the eigenvalues  $\sigma$  of the preconditioned system depends on the parameters  $z_1$  and  $z_2$ . The eigenvalues  $\sigma$  of the preconditioned matrix are solutions of the generalized eigenproblem

$$(15) \quad (L - z_1M)x = \sigma(L - z_2M)x.$$

It is easy to see that the matrices  $(L - z_1M)$  and  $(L - z_2M)$  share the same eigenvectors, which are the eigenvectors of

$$(16) \quad Lx = \lambda Mx.$$

Since for our problem  $L$  is symmetric positive semidefinite and  $M$  symmetric positive definite, the eigenvalues  $\lambda$  are real and nonnegative. Substitution of  $\lambda Mx$  for  $Lx$  in (15) yields

$$(\lambda - z_1)Mx = \sigma(\lambda - z_2)Mx,$$

and hence

$$(17) \quad \lambda - z_1 = \sigma(\lambda - z_2),$$

which, if  $z_2 \neq \lambda$ , gives

$$(18) \quad \sigma = \frac{\lambda - z_1}{\lambda - z_2}.$$

Note that if  $z_2$  coincides with an eigenvalue of (16), i.e., if  $z_2 = \lambda$ , the preconditioner  $P = L - z_2 M$  will be singular, which is a situation that has to be avoided. So in the following we assume that  $z_2 \neq \lambda$  for all eigenvalues of (16). The eigenvalues  $\lambda$  can be considered as a real parameterization of the curves (18) in the complex plane on which the eigenvalues  $\sigma$  of the preconditioned system are located.

To determine these curves we write  $\sigma = \sigma^r + i\sigma^i$  and substitute this into (17), which yields

$$\lambda - \alpha_1 - i\beta_1 = \sigma^r(\lambda - \alpha_2) - i\sigma^r\beta_2 + i\sigma^i(\lambda - \alpha_2) + \sigma^i\beta_2.$$

We can split this equation into an equation for the real terms and one for the imaginary terms:

$$\lambda - \alpha_1 = \sigma^r(\lambda - \alpha_2) + \sigma^i\beta_2,$$

$$-\beta_1 = -\sigma^r\beta_2 + \sigma^i(\lambda - \alpha_2).$$

If  $\beta_1 = \sigma^r\beta_2$ , the second equation reduces to  $\sigma^i = 0$ . If this is not the case, we get for  $\lambda$  that

$$\lambda = \alpha_2 + \frac{\sigma^r\beta_2 - \beta_1}{\sigma^i}.$$

Substitution of  $\lambda$  in the equation for the real terms yields the following result:

$$(19) \quad \beta_2(\sigma^r)^2 - (\beta_1 + \beta_2)\sigma^r + \beta_2(\sigma^i)^2 + (\alpha_1 - \alpha_2)\sigma^i = -\beta_1.$$

This equation is valid for all values of  $\alpha_1, \beta_1, \alpha_2$ , and  $\beta_2$ , including the case  $\beta_1 = \sigma^r\beta_2$ .

In the following we will distinguish between the cases  $\beta_2 = 0$  and  $\beta_2 \neq 0$ . Theorem 3.1 deals with the case  $\beta_2 = 0$ .

**THEOREM 3.1.** *Let  $\beta_2 = 0$ , let  $L$  be a symmetric positive semidefinite real matrix, and let  $M$  be a symmetric positive definite real matrix. Then the eigenvalues  $\sigma = \sigma^r + i\sigma^i$  of (15) are located on the straight line in the complex plane given by*

$$(20) \quad -\beta_1\sigma^r + (\alpha_1 - \alpha_2)\sigma^i + \beta_1 = 0.$$

*Proof.* The result follows directly from substituting  $\beta_2 = 0$  in (19).  $\square$

The next theorem characterizes the spectrum in the case when  $\beta_2 \neq 0$ .

**THEOREM 3.2.** *Let  $\beta_2 \neq 0$ , let  $L$  be a symmetric positive semidefinite real matrix, and let  $M$  be a symmetric positive definite real matrix. Then the eigenvalues  $\sigma = \sigma^r + i\sigma^i$  of (15) are located on the circle given by*

$$(21) \quad \left(\sigma^r - \frac{\beta_2 + \beta_1}{2\beta_2}\right)^2 + \left(\sigma^i - \frac{\alpha_2 - \alpha_1}{2\beta_2}\right)^2 = \frac{(\beta_2 - \beta_1)^2 + (\alpha_2 - \alpha_1)^2}{(2\beta_2)^2}.$$

The center  $c$  of this circle is

$$c = \left(\frac{\beta_2 + \beta_1}{2\beta_2}, \frac{\alpha_2 - \alpha_1}{2\beta_2}\right)$$

and the radius  $R$  is

$$R = \sqrt{\frac{(\beta_2 - \beta_1)^2 + (\alpha_2 - \alpha_1)^2}{(2\beta_2)^2}}.$$

*Proof.* Divide (19) by  $(2\beta_2)$  and complete the square.  $\square$

To understand the convergence of iterative methods it is important to know if the origin is enclosed by the circle given in Theorem 3.2. The following theorem gives a simple condition that determines this.

**THEOREM 3.3.** *If  $\beta_1\beta_2 > 0$ , the origin is not enclosed by the circle (21) given in Theorem 3.2.*

*Proof.* The origin is not enclosed by the circle if the distance of the center to the origin is larger than the radius. Hence

$$\frac{(\beta_2 + \beta_1)^2 + (\alpha_2 - \alpha_1)^2}{(2\beta_2)^2} > \frac{(\beta_2 - \beta_1)^2}{(2\beta_2)^2} + \frac{(\alpha_2 - \alpha_1)^2}{(2\beta_2)^2},$$

which is clearly the case.  $\square$

*Remark.* The center of the circle can also be written as

$$c = \frac{z_1 - \bar{z}_2}{z_2 - \bar{z}_2}$$

and the radius as

$$R = \left| \frac{z_2 - z_1}{z_2 - \bar{z}_2} \right|.$$

**3.2. The spectrum of the preconditioned Helmholtz operator with the Sommerfeld condition.** We will now study the general damped Helmholtz operator  $L + iC - z_1M$ . As before,  $L$  and  $C$  are symmetric positive semidefinite matrices,  $M$  is a symmetric and positive definite matrix, and  $z_1$  is a complex number. For our problem, the matrix  $C$  stems either from the discretization of the Sommerfeld boundary condition or from damping that does not satisfy (10). This means, for example, that a damping matrix that stems from an absorbing layer is also covered by the theory below. We consider a shifted Laplace preconditioner, i.e., a matrix of the form  $L + iC - z_2M$ , to precondition the Helmholtz operator. The eigenvalues of this matrix are given by

$$(22) \quad (L + iC - z_1M)x = \sigma_S(L + iC - z_2M)x.$$

Let  $\lambda_S$  be an eigenvalue of the generalized problem

$$(23) \quad (L + iC)x = \lambda_S Mx.$$

As in the previous section it is straightforward to show that (22) and (23) share the same eigenvectors  $x$  and that the eigenvalues  $\sigma_S$  of the preconditioned system are related to the eigenvalues  $\lambda_S$  by

$$(24) \quad (\lambda_S - z_2)\sigma_S = \lambda_S - z_1.$$

The main difference from the previous section is that  $\lambda_S$  is *complex*, whereas  $\lambda$  in the previous section was real, which allowed us to consider  $\lambda$  as a real valued parameterization of a curve in the complex plane. Although the eigenvalues  $\sigma_S$  will in general not be located on a straight line or on a circle in the complex plane if  $\lambda_S$  is complex, it is still possible to establish useful results regarding the location of  $\sigma_S$ . To this end, we will distinguish between the three cases  $\beta_2 = 0$ ,  $\beta_2 > 0$ , and  $\beta_2 < 0$ . Before we proceed we will formulate the following lemma that we will need in the remainder of this section.

LEMMA 3.1. *Let  $L$  and  $C$  be symmetric positive semidefinite real matrices and let  $M$  be a symmetric positive definite real matrix. Then the eigenvalues  $\lambda_S = \lambda_S^r + i\lambda_S^i$  of the generalized eigenproblem (23) have a nonnegative imaginary part.*

*Proof.* We use the fact that any matrix can be split into two Hermitian matrices:

$$(25) \quad A = \frac{1}{2}(A + A^H) + i\frac{1}{2i}(A - A^H) = \Re(A) + i\Im(A),$$

where

$$(26) \quad \Re(A) = \frac{1}{2}(A + A^H) \quad \text{and} \quad \Im(A) = \frac{1}{2i}(A - A^H) .$$

According to Bendixon’s theorem (see, e.g., [6, page 69]), we have

$$\lambda_{\min}^{\Re(A)} \leq \text{Re}(\lambda^A) \leq \lambda_{\max}^{\Re(A)},$$

$$\lambda_{\min}^{\Im(A)} \leq \text{Im}(\lambda^A) \leq \lambda_{\max}^{\Im(A)} .$$

The eigenvalues  $\lambda_S$  of the generalized problem (23) are also solutions of the standard eigenproblem

$$U^{-1}(L + iC)U^{-T}y = \lambda_S y$$

in which  $M = UU^T$ . This means that we can take  $A = U^{-1}(L + iC)U^{-T}$ , in which case  $\text{Im}(A) = U^{-1}CU^{-T}$ . This latter matrix is positive semidefinite, so by Bendixon’s theorem we have  $\lambda_S^i \geq 0$ .  $\square$

As in the previous section we first consider the case  $\beta_2 = 0$ .

THEOREM 3.4. *Let  $\beta_2 = 0$ , let  $L$  and  $C$  be symmetric positive semidefinite real matrices, and let  $M$  be a symmetric positive definite real matrix. Then the eigenvalues  $\sigma_S = \sigma_S^r + i\sigma_S^i$  of (22) are located in the half-plane*

$$-\beta_1\sigma_S^r + (\alpha_1 - \alpha_2)\sigma_S^i + \beta_1 \geq 0.$$

*Proof.* Since  $\beta_2 = 0$  we have

$$(\lambda_S - \alpha_2)\sigma_S = \lambda_S - z_1.$$

Splitting this equation into an equation for the real terms and one for the imaginary terms yields

$$\lambda_S^r\sigma_S^r - \lambda_S^i\sigma_S^i - \alpha_2\sigma_S^r = \lambda_S^r - \alpha_1$$

and

$$\lambda_S^r\sigma_S^i + \lambda_S^i\sigma_S^r - \alpha_2\sigma_S^i = \lambda_S^i - \beta_1.$$

The second equation gives that either  $\sigma_S^i = 0$  or

$$\lambda_S^r = \alpha_2 - \frac{\beta_1}{\sigma_S^i} + \lambda_S^i \frac{1 - \sigma_S^r}{\sigma_S^i}.$$

Substitution in the first equation and some straightforward manipulations yield

$$-\beta_1\sigma_S^r + (\alpha_1 - \alpha_2)\sigma_S^i + \beta_1 = \lambda_S^i((\sigma_S^r - 1)^2 + \sigma_S^{i2}).$$

By Lemma 3.1,  $\lambda_S^i \geq 0$ , and hence the right-hand side term is greater than or equal to zero.  $\square$

If  $\beta_2 < 0$ , the spectrum of the preconditioned matrix is characterized by Theorem 3.5.

**THEOREM 3.5.** *Let  $\beta_2 < 0$ , let  $L$  and  $C$  be symmetric positive semidefinite real matrices, and let  $M$  be a symmetric positive definite real matrix. Then the eigenvalues  $\sigma_S$  of (22) are either inside or on the circle with center  $c = \frac{z_1 - \bar{z}_2}{z_2 - \bar{z}_2}$  and radius  $R = \left| \frac{z_2 - z_1}{z_2 - \bar{z}_2} \right|$ .*

*Proof.* We have to prove that  $|\sigma_S - c| \leq R$  if  $\beta_2 < 0$ :

$$\begin{aligned}
 |\sigma_S - c| &= \left| \frac{\lambda_S - z_1}{\lambda_S - z_2} - \frac{z_1 - \bar{z}_2}{z_2 - \bar{z}_2} \right|, \\
 &= \left| \frac{(\lambda_S - z_1)(z_2 - \bar{z}_2) - (\lambda_S - z_2)(z_1 - \bar{z}_2)}{(\lambda_S - z_2)(z_2 - \bar{z}_2)} \right|, \\
 &= \left| \frac{\lambda_S(z_2 - z_1) + (z_1 - z_2)\bar{z}_2}{(\lambda_S - z_2)(z_2 - \bar{z}_2)} \right|, \\
 &= \left| \frac{\lambda_S - \bar{z}_2}{\lambda_S - z_2} \frac{z_2 - z_1}{z_2 - \bar{z}_2} \right|, \\
 (27) \qquad &= \left| \frac{\lambda_S - \bar{z}_2}{\lambda_S - z_2} \right| R.
 \end{aligned}$$

What is left to prove is that  $\left| \frac{\lambda_S - \bar{z}_2}{\lambda_S - z_2} \right| \leq 1$ . Writing

$$\lambda_S = \lambda_S^r + i\lambda_S^i$$

we get

$$(28) \qquad \left| \frac{\lambda_S - \bar{z}_2}{\lambda_S - z_2} \right|^2 = \frac{(\lambda_S^r - \alpha_2)^2 + (\lambda_S^i + \beta_2)^2}{(\lambda_S^r - \alpha_2)^2 + (\lambda_S^i - \beta_2)^2}.$$

Since  $\beta_2 < 0$  and by Lemma 3.1,  $\lambda_S^i \geq 0$ , we have

$$\frac{(\lambda_S^r - \alpha_2)^2 + (\lambda_S^i + \beta_2)^2}{(\lambda_S^r - \alpha_2)^2 + (\lambda_S^i - \beta_2)^2} \leq 1,$$

and hence the above condition is satisfied.  $\square$

If  $\beta_2 > 0$ , the spectrum of the preconditioned matrix is characterized by Theorem 3.6.

**THEOREM 3.6.** *Let  $\beta_2 > 0$ , let  $L$  and  $C$  be symmetric positive semidefinite real matrices, and let  $M$  be a symmetric positive definite real matrix. Then the eigenvalues  $\sigma_S$  of (22) are either outside or on the circle with center  $c = \frac{z_1 - \bar{z}_2}{z_2 - \bar{z}_2}$  and radius  $R = \left| \frac{z_2 - z_1}{z_2 - \bar{z}_2} \right|$ .*

*Proof.* This is analogous to the proof of Theorem 3.5.  $\square$

*Remark.* The results presented above specify regions in the complex plane where the eigenvalues of the preconditioned matrix are located. These regions are completely determined by the parameters  $z_1$  and  $z_2$ . Given the definition of  $z_1$ , (13), these regions depend only on the frequency  $f$ , on the damping parameter  $\nu$ , and of course on the shift for the preconditioner  $z_2$ . It is important to note that the regions in the complex plane where the eigenvalues are located do not depend on other physical parameters, such as the sound speed or density, nor on computational parameters, such as the size of the matrix, or on the mesh size  $h$ .

**4. Combination of the results of the spectral analysis with an upper bound on the GMRES-residual norm.** In this section we will combine the results of the spectral analysis presented in the previous section with a well-known upper bound on the GMRES-residual norm. This upper bound assumes that the spectrum is enclosed by a circle, and hence this bound can be naturally combined with the circle specified in Theorems 3.2 and 3.5.

Let the eigenvalues of the preconditioned matrix be enclosed by a circle with radius  $R$  and center  $c$  as in Theorem 3.5. Then the GMRES-residual norm after  $k$  iterations  $\|r^k\|$  satisfies (see, e.g., [12])

$$(29) \quad \frac{\|r^k\|}{\|r^0\|} \leq c_2(X) \left( \frac{R}{|c|} \right)^k.$$

In this equation  $X$  is the matrix of eigenvectors and  $c_2(X)$  its condition number in the 2-norm. If this condition number is large, the upper bound gives no information about the convergence, since in that case there is no relation between the location of the eigenvalues and the convergence behavior of the preconditioned Krylov method [5]. Fortunately, in our application we may expect that the condition number of the eigenvector matrix is relatively small. If  $C = 0$ , the eigenvectors of the preconditioned matrix are the same as in (16), and hence independent of the shift parameters. Moreover, since the eigenvectors of (16) are  $M$ -orthogonal and  $M$  is a (scaled) mass matrix, which is in general well conditioned, we expect that  $c_2(X)$  will be small in practice. This can be seen from

$$X^T M X = I \Leftrightarrow c_2(X^T M X) = 1 \Leftrightarrow c_2(M^{\frac{1}{2}} X) = 1.$$

Since

$$c_2(X) = c_2(M^{-\frac{1}{2}} M^{\frac{1}{2}} X) \leq c_2(M^{-\frac{1}{2}}) c_2(M^{\frac{1}{2}} X),$$

we get

$$c_2(X) \leq \sqrt{c_2(M)}.$$

If  $C \neq 0$ , the eigenvectors of the preconditioned system are the same as of (23). These are unfortunately not  $M$ -orthogonal, but for many problems we can consider (23) as a relatively small perturbation of (16), in which case we can still expect that  $c_2(X)$  is small.

**4.1. Optimization of the shift.** Although (29) gives only an upper bound on the GMRES-residual norm, it allows us to derive a “quasi” optimal choice for the shift. We derive this shift by minimizing the upper bound. For this it is sufficient to minimize the ratio  $\frac{R}{|c|}$ , or, using Theorem 3.5, the function

$$f(\alpha_2, \beta_2) = \frac{R^2}{|c|^2} = \frac{(\alpha_2 - \alpha_1)^2 + (\beta_2 - \beta_1)^2}{(\alpha_2 - \alpha_1)^2 + (\beta_2 + \beta_1)^2}.$$

To analyze this function we differentiate with respect to  $\alpha_2$ ,

$$\frac{\partial f}{\partial \alpha_2} = \frac{8(\alpha_2 - \alpha_1)\beta_1\beta_2}{((\alpha_2 - \alpha_1)^2 + (\beta_2 + \beta_1)^2)^2},$$

and with respect to  $\beta_2$ ,

$$\frac{\partial f}{\partial \beta_2} = \frac{4\beta_1((\beta_2^2 - \beta_1^2) - (\alpha_2 - \alpha_1)^2)}{((\alpha_2 - \alpha_1)^2 + (\beta_2 + \beta_1)^2)^2}.$$

Clearly, both derivatives are zero at  $\alpha_1 = \alpha_2, \beta_1 = \beta_2$ . This choice for the shift minimizes of course the upper bound since this corresponds to using the original operator as a preconditioner, which means that performing the preconditioning operation is as hard as solving the original system.

We are interested in the case when the preconditioning operation is relatively cheap. In particular, we have in mind the situation when preconditioning operations can be efficiently carried out using a fixed number of cycles of a multigrid method for the whole range of shifts under consideration. We therefore restrict our analysis to values for the shift for which multigrid is known to work well. We first consider the purely imaginary shift [2, 3, 4]; this means that  $\alpha_2$  equals zero. In this case, the derivative with respect to  $\beta_2$  is zero if

$$(30) \quad (\beta_2^2 - \beta_1^2) - \alpha_1^2 = 0,$$

yielding

$$\beta_2 = \pm|z_1|.$$

Since by (13)  $\beta_1 = -(2\pi f)^2\nu \leq 0$ , we must choose by Theorem 3.3  $\beta_2 \leq 0$ , and hence  $z_2 = -|z_1|i$  as the shift that minimizes the upper bound (29). This choice is also optimal if we consider all possible shifts for which  $\alpha_2 \leq 0$ , meaning all possible shifts for which the preconditioner has all its eigenvalues in the right half-plane. By (13),  $\alpha_1 = (2\pi f)^2 > 0$ , and by Theorem 3.3,  $\beta_1\beta_2 \geq 0$ , so  $\frac{\partial f}{\partial \alpha_2}$  is negative for  $\alpha_2 \leq 0$ . Therefore  $f(\alpha_2, \beta_2)$  takes its minimum on the edge  $\alpha_2 = 0$ . We conclude that the choice

$$(31) \quad z_2 = -|z_1|i$$

minimizes the upper bound (29) for all  $z_2 \in \mathbb{C}$ , with  $\alpha_2 \leq 0$ .

The same methodology for deriving an optimal shift can still be used if we do not restrict ourselves to the case  $\alpha_2 \leq 0$ . Such a shift still (approximately) minimizes the number of GMRES iterations. However, the performance of a multigrid method for the preconditioning operations will deteriorate if  $z_2$  is too close to  $z_1$ , and hence such a shift would no longer minimize the total work of the whole solution process. How to find a shift that minimizes the total work, if the performance of multigrid depends on the shift, is of great practical importance, but is outside the scope of this paper.

**4.2. Discussion.** The upper bound (29) is meaningful only if the circle does not enclose the origin. This is the case if  $\beta_1 < 0$ , or equivalently if  $\nu > 0$ . However, because of continuity arguments, result (31) for the “quasi” optimal shift is still valid if  $\beta_1 = 0$ .

As was remarked in the previous section, the circle around the spectrum of the preconditioned matrix depends only on  $z_2$ , on  $f$ , and on  $\nu$ . Consequently, if  $\beta_1 < 0$ , inequality (29) yields an upper bound on the GMRES-residual norm that also depends only on the frequency  $f$  and on the damping parameter  $\nu$ . Because of this, the number of GMRES iterations should be bounded from above by a constant that is independent of the mesh size.

By scaling the shift  $z_2$  with the frequency we can make the upper bound on the number of GMRES iterations also independent of frequency. To this end we introduce the scaled shift

$$\tilde{z}_2 = \tilde{\alpha}_2 + i\tilde{\beta}_2 = \frac{z_2}{(2\pi f)^2}.$$

Applying Theorem 3.5 and substituting  $z_2 = (2\pi f)^2 \tilde{z}_2$  and the definition for  $z_1$  (13) into (29) yield

$$(32) \quad \frac{\|r^k\|}{\|r^0\|} \leq c_2(X) \left(\frac{R}{|c|}\right)^k = c_2(X) \sqrt{\frac{(\tilde{\alpha}_2 - 1)^2 + (\tilde{\beta}_2 + \nu)^2}{(\tilde{\alpha}_2 - 1)^2 + (\tilde{\beta}_2 - \nu)^2}}.$$

Clearly, this upper bound depends only on the damping parameter  $\nu$  and on the choice for the parameter  $\tilde{z}_2$ .

**5. Experiments.** In this section we describe a typical test problem with a variable sound velocity. The location of the eigenvalues of the discretized operators are compared with the theoretically predicted locations. The value of the optimal shift is validated by numerical experiments. Finally, it appears that the convergence behavior of GMRES is independent of the mesh size.

**5.1. Description of the test problem.** The test problem that we consider mimics three layers with a simple heterogeneity and is taken from [11].

For  $\nu \in \mathbb{R}$ , find  $p \in \mathbb{C}^N$  satisfying

$$(33) \quad \begin{cases} -\Delta p - (1 - \nu)\left(\frac{2\pi f}{c(\mathbf{x})}\right)^2 p = s & \text{in } \Omega = (0, 600) \times (0, 1000) \text{ meter}^2, \\ s = \delta(x_1 - 300, x_2), \quad x_1 = (0, 600), \quad x_2 = (0, 1000) \\ \text{with Sommerfeld conditions or Neumann conditions on } \Gamma \equiv \partial\Omega. \end{cases}$$

The local sound velocity is given as in Figure 1. The density is assumed to be constant.

We have discretized the above problem with the finite element method using linear triangular elements. The computations that are described in this section have been performed with MATLAB.

**5.2. Location of the eigenvalues.** The first experiments validate the theorems that are presented in section 3. To this end we have taken as source frequency  $f = 2$  and we have discretized the problem with mesh size  $h = 100/2$ . We have calculated all the eigenvalues of the preconditioned matrix for four typical combinations of values of the scaled parameters  $\tilde{z}_1$  and  $\tilde{z}_2$ . (See Figure 2.) The upper left-hand side subplot shows the spectrum of the preconditioner if a real shift is chosen, as suggested in [8]. As was predicted by Theorem 3.1, the eigenvalues for the Neumann problem, which are indicate with the symbol \*, are located on a line. Since the example contains damping, the line does not pass through the origin. The eigenvalues of the Sommerfeld problem, which are indicated with the symbol o, are all on one side of the line, as is predicted by Theorem 3.4. Note that the eigenvalues move away from the origin if the Neumann problem is replaced with the Sommerfeld problem.

The upper right-hand side subplot shows the spectrum of the preconditioner if a purely imaginary shift is chosen. The eigenvalues of the Neumann problem are located on the circle that is given by Theorem 3.2, and the eigenvalues of the Sommerfeld problem are, as predicted by Theorem 3.5, either on or inside this circle. This example does not contain damping (apart from the radiation condition):  $\tilde{z}_1$  is real. Consequently, the circle contains the origin.

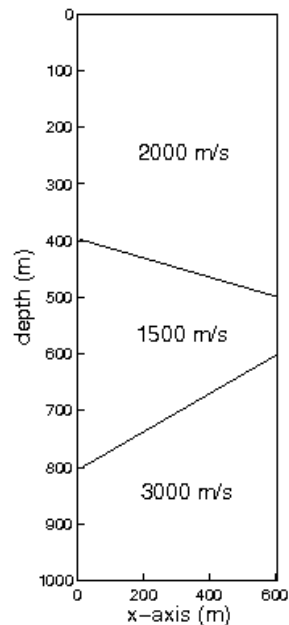


FIG. 1. Problem geometry with sound velocity profile.

The lower left-hand side subplot shows another picture of the spectrum of the preconditioner if a purely imaginary (negative) shift is chosen. In this case the problem contains damping since  $\tilde{z}_1$  is complex. As a result, the circle is smaller than for the previous example, and the origin is outside the circle.

The lower right-hand side subplot shows for the same  $z_1$  what happens if the sign of the complex shift is wrongly (i.e., positively) chosen. According to Theorem 3.6 the eigenvalues of the Sommerfeld problem should in this case be either on or outside the circle. This is confirmed by the numerical results. Moreover, by Theorem 3.3, the origin should be enclosed by the circle, which is the case.

**5.3. Optimization of the shift.** The second group of experiments validates the optimal value for the shift  $z_2$  that was found in section 4. This value is given by (31).

The optimal value was determined by minimizing the ratio  $\frac{R}{|c|}$ . Using the scaled variables  $\tilde{z}_2 = z_2/(2\pi f)^2$ , this ratio can be written as

$$(34) \quad \frac{R}{|c|} = \sqrt{\frac{(\tilde{\alpha}_2 - 1)^2 + (\tilde{\beta}_2 + \nu)^2}{(\tilde{\alpha}_2 - 1)^2 + (\tilde{\beta}_2 - \nu)^2}}.$$

This function takes values between 0 and 1. A small value of  $\frac{R}{|c|}$  indicates fast convergence and a value close to 1 slow convergence. Figure 3 shows, for three different damping parameters  $\nu$ , how the value of  $\frac{R}{|c|}$  depends on  $\tilde{\alpha}_2$  and  $\tilde{\beta}_2$ . The values on the contour lines correspond to the value of  $\frac{R}{|c|}$ . The three plots show clearly that (34) takes its minimum when  $\tilde{\alpha}_2 = 0$ , and that the optimal  $\tilde{\beta}_2$  becomes more negative when the damping parameter is increased. These observations are of course consistent with the optimal value for the shift parameter (31) that was derived in section 4.

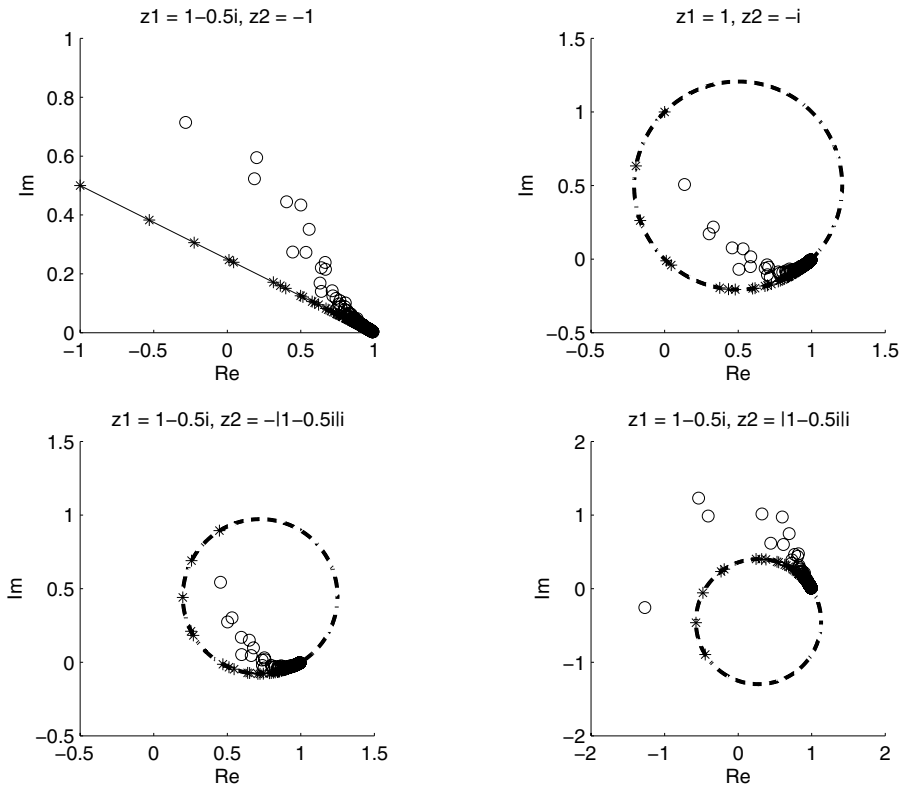


FIG. 2. Spectra for different values of the complex shift in the preconditioner;  $h = 100/2, f = 2$ . The symbol \* denotes eigenvalues for the Neumann problem; o denotes eigenvalues for the Sommerfeld problem.

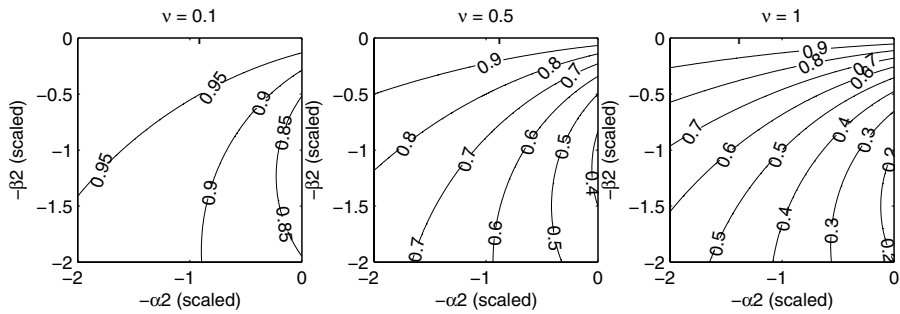


FIG. 3. Contour plot of the convergence factor as a function of the complex shift.

To validate that this value is really (sub-) optimal in actual computations we solve the Sommerfeld problem with scaled imaginary shifts ranging from 0 to  $-2$ . For the mesh size we take  $h = 100/8$  and perform the experiment for four different damping parameters. The result is shown in Figure 4. Clearly, the more damping, the fewer the number of GMRES iterations, and the larger (more negative) the optimal imaginary shift.

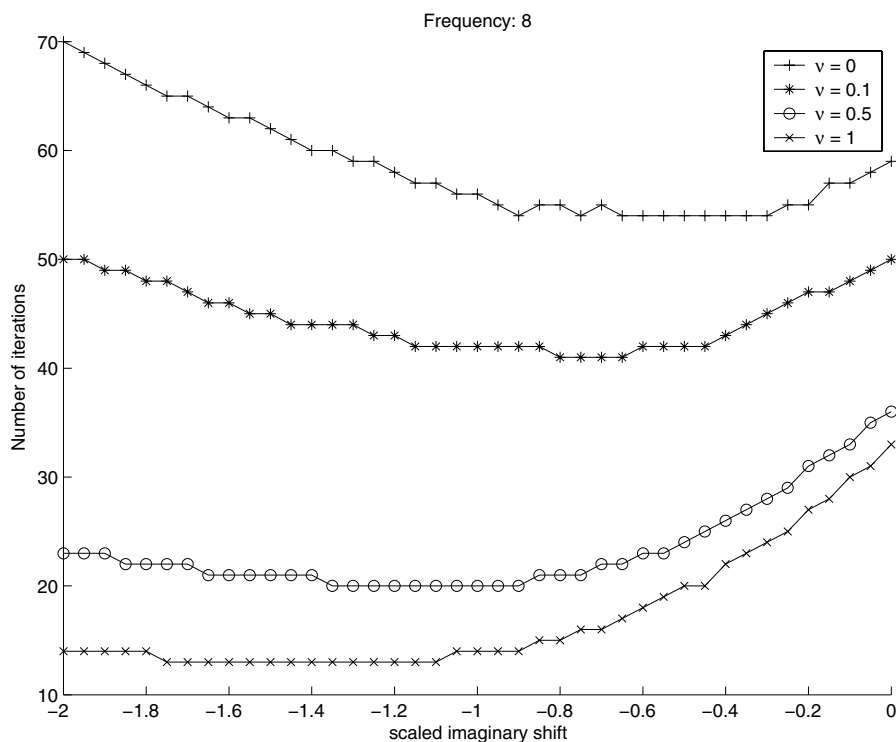


FIG. 4. Actual number of iteration as a function of the imaginary shift ( $h = 100/8$ ).

TABLE 1  
Number of iterations for “optimal” shift and minimum number of iterations.

Damping	Optimal shift	Iterations “optimal” shift	Min. number of iterations
$\nu = 0$	1	56	54
$\nu = 0.1$	1.005	42	41
$\nu = 0.5$	1.118	20	20
$\nu = 1$	1.4142	13	13

Table 1 shows the minimum number of iterations and compares this with the number of iterations when the “optimal” shift (31) is used. The results show that the shift (31) is nearly optimal with respect to the number of GMRES iterations.

**5.4. Mesh dependency.** The last set of experiments examines the dependency of the number of iterations of preconditioned GMRES on the mesh size.

Table 2 shows for an increasingly fine step size  $h$  the number of iterations for the Sommerfeld problem. The experiment is performed for four different damping parameters, and the frequency is kept fixed to  $f = 2$ . The results show that for all four different values of the damping parameter the number of iterations is independent of the step size  $h$ . Based on the discussion at the end of section 4, this could be expected. The theory that is presented in section 4, however, does not make any predictions about the mesh-dependent performance of preconditioned GMRES for problems with a zero damping parameter.

The results of the same type of experiments, but now with a frequency that scales

TABLE 2  
*Number of iterations under mesh refinement for a fixed frequency.*

	Number of iterations				
$h :$	100/2	100/4	100/8	100/16	100/32
$f :$	2	2	2	2	2
$\nu = 0$	14	13	13	13	13
$\nu = 0.1$	13	12	12	12	13
$\nu = 0.5$	11	10	11	11	11
$\nu = 1$	9	9	9	9	9

TABLE 3  
*Number of iterations under mesh refinement for increasingly high frequencies.*

	Number of iterations				
$h :$	100/2	100/4	100/8	100/16	100/32
$f :$	2	4	8	16	32
$\nu = 0$	14	25	56	116	215
$\nu = 0.1$	13	22	42	63	80
$\nu = 0.5$	11	16	20	23	23
$\nu = 1$	9	11	13	13	13

with the mesh size, are tabulated in Table 3. These results confirm that if the damping parameter is nonzero, the number of GMRES iterations is bounded by a number that is independent of the mesh size. This is most apparent in the results for  $\nu = 0.5$  and  $\nu = 1$ . The results for  $\nu = 0$  seem to indicate that the number of GMRES iterations more or less doubles if the step size is halved. As was remarked above, the theory presented in section 4 does not make any predictions for the case when  $\nu = 0$ .

To check that  $c_2(X)$  is actually small for the above test cases we have also computed the condition numbers of the mass matrices on the five meshes. These condition numbers are equal to 24 for all meshes; hence we have that

$$c_2(X) \leq \sqrt{c_2(M)} = 2\sqrt{3}.$$

**6. Conclusions.** We have presented a spectral analysis of the Helmholtz operator that is preconditioned with a shifted Laplace operator. We have shown that, depending on the value of the shift, the eigenvalues of the preconditioned matrix are located either in or on a circle, or in a half-plane. Combining these results concerning the spectrum of the preconditioned matrix with a well-known bound on the GMRES-residual norm allowed us to determine a close-to-optimal shift. Furthermore, we have shown for problems with a nonzero damping parameter that there is an upper bound on the number of GMRES iterations that depends only on the damping parameter and hence is independent of the mesh size, the frequency, the sound speed, and the density.

We have derived the close-to-optimal shift for the shifted-Laplace preconditioner in combination with GMRES under the assumption that preconditioning operations are performed exactly. In practice, however, preconditioning operations are performed approximately, for example, using a multigrid method, and another Krylov method, such as Bi-CGSTAB [14], may be used instead of GMRES. In this case the analysis that has been presented in this paper no longer holds. However, experimental results reported in [3], where Bi-CGSTAB is used as a Krylov solver and preconditioning operations are performed approximately with one multigrid cycle, use values for the shift that are close to the predicted value for the optimal shift we present in this

paper. The experimental results are also in these cases quite satisfactory. We therefore conclude that our results provide strong guidelines on how to select the shift parameter for all Krylov methods, as well as for approximate preconditioners.

**Acknowledgments.** The authors thank Kees Oosterlee for valuable discussions.

## REFERENCES

- [1] A. BAYLISS, C. I. GOLDSTEIN, AND E. TURKEL, *An iterative method for the Helmholtz equation*, J. Comput. Phys., 49 (1983), pp. 443–457.
- [2] Y. A. ERLANGGA, C. VUIK, AND C. W. OOSTERLEE, *On a class of preconditioners for the Helmholtz equation*, Appl. Numer. Math., 50 (2005), pp. 409–425.
- [3] Y. A. ERLANGGA, C. W. OOSTERLEE, AND C. VUIK, *Comparison of multigrid and incomplete LU shifted-Laplace preconditioners for the inhomogeneous Helmholtz equation*, Appl. Numer. Math., 56 (2006), pp. 648–666.
- [4] Y. A. ERLANGGA, C. W. OOSTERLEE, AND C. VUIK, *A novel multigrid based preconditioner for heterogeneous Helmholtz problems*, SIAM J. Sci. Comput., 27 (2006), pp. 1471–1492.
- [5] A. GREENBAUM, V. PTÁK, AND Z. STRAKOŠ, *Any nonincreasing convergence curve is possible for GMRES*, SIAM J. Matrix Anal. Appl., 17 (1996), pp. 465–469.
- [6] A. S. HOUSEHOLDER, *The Theory of Matrices in Numerical Analysis*, Blaisdell Publishing Company, New York, 1964.
- [7] R. KECHROUD, A. SOULAIMANI, AND Y. SAAD, *Preconditioning techniques for the solution of the Helmholtz equation by the finite element method*, in Computational Science and Its Applications (ICCSA 2003), Part II, Lecture Notes in Comput. Sci. 2668, V. Kumar et al., eds., Springer, Berlin, 2003, pp. 847–858.
- [8] A. L. LAIRD AND M. B. GILES, *Preconditioned Iterative Solution of the 2D Helmholtz Equation*, Tech. Report 02/12, Oxford Computer Laboratory, Oxford, UK, 2002.
- [9] A. L. LAIRD AND M. B. GILES, *Preconditioning harmonic unsteady potential flow calculations*, AIAA J., 44 (2006), pp. 2654–2662.
- [10] T. A. MANTEUFFEL AND S. V. PARTER, *Preconditioning and boundary conditions*, SIAM J. Numer. Anal., 27 (1990), pp. 656–694.
- [11] R. E. PLESSIX AND W. A. MULDER, *Separation-of-variables as a preconditioner for an iterative Helmholtz solver*, Appl. Numer. Math., 44 (2003), pp. 385–400.
- [12] Y. SAAD AND M. H. SCHULTZ, *GMRES: A generalized minimal residual algorithm for solving nonsymmetric linear systems*, SIAM J. Sci. Stat. Comput., 7 (1986), pp. 856–869.
- [13] E. TURKEL, *Numerical methods and nature*, J. Sci. Comput., 28 (2006), pp. 549–570.
- [14] H. A. VAN DER VORST, *Bi-CGSTAB: A fast and smoothly converging variant of Bi-CG for the solution of nonsymmetric linear systems*, SIAM J. Sci. Stat. Comput., 13 (1992), pp. 631–644.